Brain Evolution Triggers Increased Diversification of Electric Fishes

Bruce A. Carlson,[1]* Saad M. Hasan,[1] Michael Hollmann,[1] Derek B. Miller,[1] Luke J. Harmon,[2] Matthew E. Arnegard[3]

Communication can contribute to the evolution of biodiversity by promoting speciation and reinforcing reproductive isolation between existing species. The evolution of species-specific signals depends on the ability of individuals to detect signal variation, which in turn relies on the capability of the brain to process signal information. Here, we show that evolutionary change in a region of the brain devoted to the analysis of communication signals in mormyrid electric fishes improved detection of subtle signal variation and resulted in enhanced rates of signal evolution and species diversification. These results show that neural innovations can drive the diversification of signals and promote speciation.

Although we assume that sensory processing is fundamentally important for the detection of species-specific communications, or "signals" (*1*), we know relatively little about how brain evolution might affect signal divergence and speciation. African electric fishes within the family Mormyridae provide an ideal model system for relating brain evolution to diversification. The >200 described species in this family are phylogenetically and phenotypically diverse (*2–8*); communicate using brief, species-specific, and easily quantified electric signals (*9*); and process these signals in a well-defined sensory pathway devoted solely to the analysis of electric communication signals (*10–12*) (fig. S1).

Mormyrids generate electric signals to communicate and to actively sense their environment (*11*). These signals have evolved more rapidly than body shape, size, and trophic ecology, suggesting that electric communication behavior has played a key role in the radiation of mormyrids (*3*). Further, playback experiments in a few species suggest that these signals are critical for species recognition during mate choice (*13–16*). Electric signals are generated by an electric organ in the tail, which consists of electrically excitable cells called electrocytes (*17*). Electrocyte stalks evolved with the origin of mormyrids, and developmental flexibility in stalk morphology arose with the origin of the subfamily Mormyrinae (*2*). This evolutionary change in the Mormyrinae established enhanced capacity for signal variation that is lacking in the Petrocephalinae, the only other mormyrid subfamily (Fig. 1).

Mormyrids have three types of electroreceptors: ampullary organs, mormyromasts, and knollenorgans (*18*). Communication behavior is mediated exclusively by knollenorgans (*10*). In a region of the midbrain called the exterolateral nucleus (EL; fig. S1), the timing of responses of knollenorgans located on different parts of the body is compared to extract information about electric signals (*10–13*). Despite the importance of the EL for signal analysis, EL anatomy has only been characterized in a few species (*10–12*). To investigate the role of brain evolution in mormyrid diversification, we performed a comparative analysis of EL anatomy. We obtained serial sections from the brains of 26 species (table S2). After standard histological processing, we delineated the borders of the EL in each section using established criteria (*12*). We then calculated total EL volume normalized to brain mass [see supporting online material (SOM)].

Previous studies identified distinct anterior and posterior subdivisions in the EL, referred to as ELa and ELp, respectively (*10*). Sixteen of the species that we studied clearly have separate ELa/ELp subdivisions (Fig. 2A). However, the
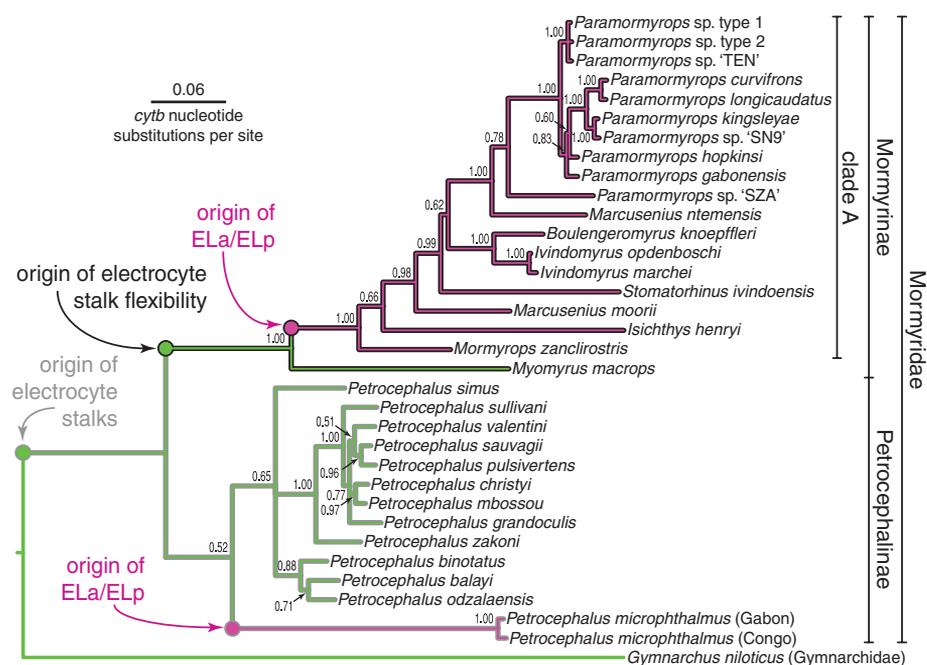
Fig. 1. Inferred tree of phylogenetic relationships among mormyrid species and morphs. The phylogeny was estimated by Bayesian analysis of *cytb* sequences (values at nodes are posterior probabilities). A sequence from the closest outgroup to the Mormyridae (*Gymnarchus niloticus*) was used to root the tree. Green branches represent a small exterolateral nucleus (EL) and magenta branches represent an enlarged EL divided into anterior and posterior subdivisions (ELa/ELp); we reconstructed ancestral states using parsimony (see text). Gray outline represents electric organs with electrocyte stalks, and black outline represents electric organs with developmentally labile stalks, based on a previous study (*2*).

[1]Department of Biology, Washington University in St. Louis, St. Louis, MO 63130, USA. [2]Department of Biological Sciences, University of Idaho, Moscow, ID 83844, USA. [3]Human Biology Division, Fred Hutchinson Cancer Research Center, Seattle, WA 98109, USA.

*To whom correspondence should be addressed. E-mail: carlson.bruce@wustl.edu

remaining 10 species have a relatively small EL without any apparent subdivisions (Fig. 2B). Within the subfamily Mormyrinae, the genus *Myomyrus* has a small EL, whereas all other genera have an enlarged and subdivided ELa/ELp (Fig. 2C and table S2). The monophyly of the latter group is strongly supported by our *cytb* phylogeny (Fig. 1), as well as several published studies that used multiple molecular markers (*2–6*), We therefore refer to this lineage as "clade A," and we conclude that all species in this lineage have an ELa/ELp (Fig. 1). Within the subfamily Petrocephalinae, we find that *Petrocephalus microphthalmus* is the only species with an enlarged ELa/ELp (Fig. 2C and table S2).

This pattern of EL anatomy suggests two equally parsimonious scenarios: Either the EL was ancestral and an enlarged ELa/ELp evolved twice independently, or ELa/ELp was ancestral, and a reduced EL evolved twice independently. To distinguish between these two possibilities, we related EL anatomy in mormyrids to a published description of midbrain anatomy in the monotypic Gymnarchidae, *Gymnarchus niloticus* (*19*), the sister taxon to all mormyrids (Fig. 1). This study identified an EL homolog without subdivisions, leading us to conclude that the EL is the ancestral mormyrid character state and that an enlarged ELa/ELp evolved twice, once at the origin of clade A and once in *P. microphthalmus* (Fig. 1).

Previous work has identified two distinct patterns of knollenorgan receptor organization:

a broad distribution of receptors throughout the body, or discrete clusters of receptors on the head (*20*). We hypothesized that this difference might relate to variation in EL anatomy. To test this hypothesis, we mapped knollenorgan locations in 15 species (see SOM) and combined our findings with published descriptions (*6, 20, 21*), yielding data on 11 clade A species, 2 *Myomyrus* species, and 13 petrocephaline species (table S2). All clade A species and *P. microphthalmus* have broad knollenorgan distributions (Fig. 3, A and B, and fig. S2B). With one exception (*Petrocephalus zakoni*), all other petrocephaline species have clusters of knollenorgans located only on the head (Fig. 3C and fig. S2C). *Myomyrus* has an intermediate phenotype, with a single cluster on the head as well as a low-density, broad distribution (Fig. 3D and fig. S2C). Thus, despite extensive interspecific variation, ELa/ELp is universally associated with a broad distribution of knollenorgans (table S2).

Mormyrids analyze electric signals in the EL by comparing the response times of knollenorgans located on different parts of the body (*10–13*), suggesting that species with broad receptor distributions should be better equipped for signal discrimination. Therefore, we hypothesized that ELa/ELp evolved to facilitate the processing of receptor responses for signal analysis, which predicts that species with an ELa/ELp should be better at detecting signal differences than species with an EL. To test our hypothesis, we performed

playback experiments in the field (see SOM). Previous research identified two distinct behavioral responses to electrosensory stimulation: increases in electric discharge rate (*22*), or pauses in electric output (*23*). We observed both responses. Among the six clade A species tested, four responded to stimulation with rate increases, and one responded with pauses. In the one remaining species (*Brienomyrus brachyistius*), two individuals responded with rate increases, and two responded with pauses. All four petrocephaline species responded with pauses.

In every species, repeated presentation of the same stimulus led to a decrease in response (i.e., habituation; fig. S4). We therefore used a habituation-dishabituation paradigm to assess signal discrimination ability in the field. Both control and experimental stimuli consisted of 10 bursts of 10 pulses each. For controls, all 100 pulses were an identical conspecific signal. Experimental stimuli were the same except that all 10 pulses in the ninth burst were a phase-shifted version of the same signal (fig. S3). Signal
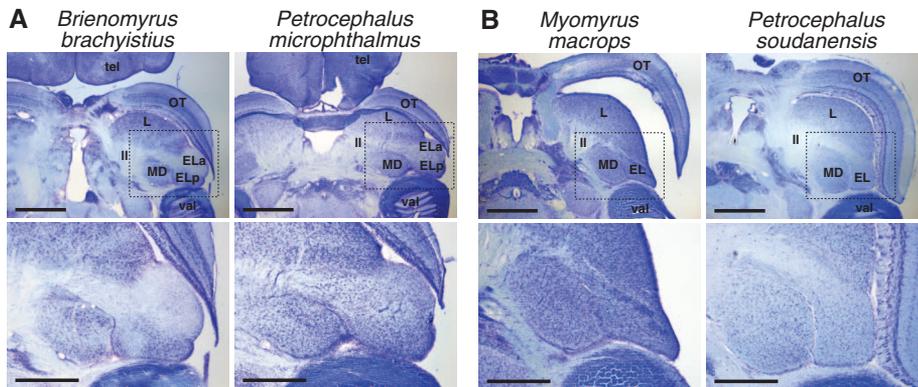
Fig. 2. Anatomy of the exterolateral nucleus (EL). (**A**) Midbrain portion of 50-μm horizontal sections from the clade A species *B. brachyistius* and the petrocephaline *P. microphthalmus*. Dashed boxes in upper images delimit enlarged images below (scale bars 1 mm and 500 μm, respectively). Both species have an enlarged EL with distinct anterior and posterior subdivisions (ELa/ELp). (**B**) The petrocephaline *P. soudanensis* and mormyrine *M. macrops* both have a small EL with no subdivisions. L, lateral nucleus; ll, lateral lemniscus; tel, telencephalon; OT, optic tectum; MD, mediodorsal nucleus; val, valvula cerebellum. (**C**) Bar graph showing the median ± range of normalized EL volumes across all taxa studied (table S2 gives sample sizes).
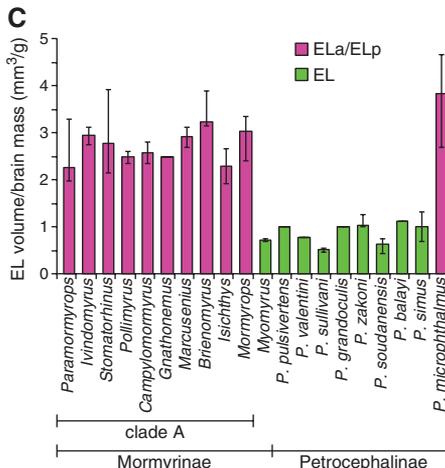
Fig. 3. An enlarged and subdivided exterolateral nucleus (ELa/ELp) is universally associated with broadly distributed knollenorgan electroreceptors. Knollenorgan locations are indicated by red dots. (**A**) *B. brachyistius* has a broad distribution of knollenorgans, as found in all clade A species. (**B**) *P. microphthalmus*, the sole petrocephaline species with an ELa/ELp, also has a broad knollenorgan distribution. (**C**) *P. soudanensis* has three knollenorgan clusters. (**D**) *M. macrops* has an intermediate pattern, with a single cluster and a low density of knollenorgans throughout the body.

discrimination was assessed as the change in response from the eighth to ninth burst. In all clade A species, inserting a phase-shifted signal into the stimulus train led to a partial recovery of response (i.e., dishabituation) (Fig. 4A; discharge rate increases: $n = 34$, $z = 4.57$, $P < 0.00001$; pauses: $n = 7$, $z = 2.37$, $P < 0.05$). The three petrocephaline species with an EL showed no evidence of discrimination (Fig. 4A; $n = 12$, $z = 1.49$, $P = 0.13$). However, in *P. microphthalmus*, the sole petrocephaline species with an ELa/ELp, the phase-shifted signal elicited dishabituation (Fig. 4A; $n = 10$, $z = 2.80$, $P < 0.01$). These results demonstrate that the independent evolution of ELa/ELp established signal discrimination abilities that are lacking in species with an EL.

Animal communication depends on both senders and receivers; in addition to the sensory capacity for signal discrimination, traits permitting the evolution of signal variation are necessary for a communication system that promotes diversification. Therefore, we hypothesized that rapid signal divergence and species diversification should be restricted to clade A, the only mormyrid lineage with both ELa/ELp and developmentally flexible electrocytes (Fig. 1).

To test the importance of these traits on rates of signal divergence, we analyzed the electric signals of species collected in two locales: the Ivindo River of Gabon (*3, 9*) and Odzala National Park of the Republic of the Congo (*5, 6*), homes to the largest known assemblages of Mormyrinae and Petrocephalinae, respectively. The combined data set represents 18 species and morphs within clade A and 13 outgroup species (fig. S5). Using cross-correlation (fig. S6) and multidimensional scaling (see SOM), we computed coordinates of all 407 signals in this data set within a two-dimensional space (Fig. 4B). We then computed squared Mahalanobis distances (D^2) between the centroids of each species or morph and plotted these values against ultrametric phylogenetic distances based on our phylogeny (Fig. 1). Assuming no particular model of evolution, the resulting plot reveals greater signal variation and more rapid signal divergence in clade A (Fig. 4C). We then formally compared signal divergence rates using a Brownian motion framework (*24*). Considering dimension 1, which reflects variation in temporal features of the signals (Fig. 4B), we found that the rate of signal divergence in clade A is more than 10 times fast-er compared to that of other mormyrids ($\sigma^2_A = 0.000417$, $\sigma^2_{other} = 0.000037$, AICc = 13.9804, $P < 0.0002$). For dimension 2, which reflects other signal features, we found a twofold higher rate of signal divergence in clade A, but the difference was not significant ($\sigma^2_A = 0.000224$, $\sigma^2_{other} = 0.000118$, AICc = −1.1484; $P = 0.25$).

To test our hypothesis that clade A has experienced higher rates of species diversification, we compared diversification rates in clade A to closely related outgroup lineages (*25*). There are at least 175 extant species in clade A (*7*). By contrast, there are only 3 known species of *Myomyrus*, and only 30 known species in the entire subfamily Petrocephalinae (*5–7*). Every family of Osteoglossomorpha outside the Mormyridae contains 10 or fewer extant species (*7*). Moreover, the only two known osteoglossomorph species flocks are restricted to clade A (*3, 5, 8*). We find statistical support for net rates of diversification in clade A that are three to five times higher than those in closely related outgroup lineages (see SOM). This result is robust across a range of possible average extinction levels (table S3), supporting our hypothesis that the evolution of ELa/ELp triggered explosive diversification in clade A compared to that of other mormyroid lineages (Fig. 1). However, this same evolutionary change in *P. microphthalmus* did not trigger rapid diversification. We propose that the lack of developmentally flexible electrocyte stalks within the Petrocephalinae (*2*) impeded rapid diversification through signal divergence in the *P. microphthalmus* lineage.

Evolution of communication systems can have profound effects on species radiation. Evolutionary change in the structure of the anuran inner ear may have fostered increased rates of speciation through its effects on vocal communication (*26*). Similarly, the adaptation of visual receptors to different light environments has contributed to cichlid speciation through its effects on mate recognition (*27, 28*). The resulting radiations of species can then lead to evolutionary divergence in brain structure as a secondary consequence of adaptation to new ecological niches (*29, 30*). Our results demonstrate the reverse relationship, in which brain evolution directly promotes diversification. We reveal that evolutionary change in the functional organization of sensory pathways can establish new perceptual abilities that trigger explosive diversification.
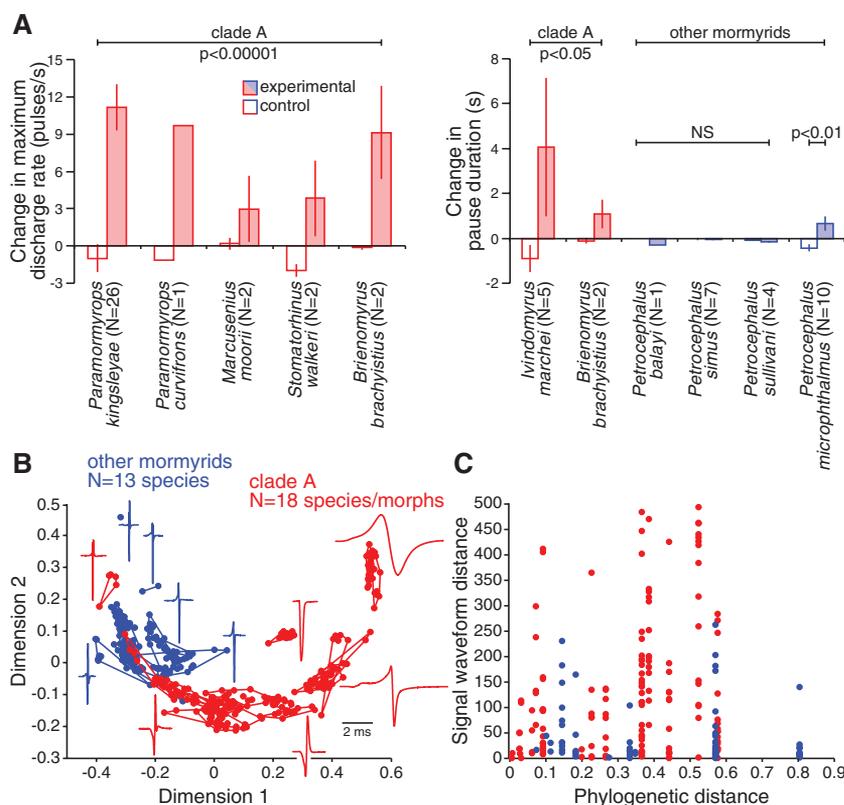

Fig. 4. Behavioral discrimination of signals and the evolution of signal diversity. (**A**) Dishabituation of behavioral responses, shown as the change in response from the eighth to ninth stimulus (mean ± SEM; see text). Species in clade A are shown in red; all other species are shown in blue. Statistical significance was assessed using Wilcoxon's matched-pairs test. (**B**) Minimum polygons enclosing species or morphs in bivariate signal space (as obtained through multidimensional scaling of signal cross-correlations; see SOM), including 11 example signals placed next to their location within this space. (**C**) Pairwise signal distances (Mahalanobis D^2) between species or morphs plotted against pairwise phylogenetic distances between *cytb* sequences.

References and Notes

1. C. J. Hoskin, M. Higgie, *Ecol. Lett.* **13**, 409 (2010).
2. J. P. Sullivan, S. Lavoué, C. D. Hopkins, *J. Exp. Biol.* **203**, 665 (2000).
3. M. E. Arnegard et al., *Am. Nat.* **176**, 335 (2010).
4. S. Lavoué, J. P. Sullivan, C. D. Hopkins, *Biol. J. Linn. Soc. Lond.* **78**, 273 (2003).
5. S. Lavoué, M. E. Arnegard, J. P. Sullivan, C. D. Hopkins, *J. Physiol. Paris* **102**, 322 (2008).
6. S. Lavoué, J. P. Sullivan, M. E. Arnegard, *Zootaxa* **2600**, 1 (2010).
7. W. N. Eschmeyer, J. D. Fong, *Catalog of Fishes* (California Academy of Sciences, San Francisco, 2010).

8. P. G. D. Feulner, F. Kirschbaum, V. Mamonekene, V. Ketmaier, R. Tiedemann, *J. Evol. Biol.* **20**, 403 (2007).
9. C. D. Hopkins, *Am. Zool.* **21**, 211 (1981).
10. M. A. Xu-Friedman, C. D. Hopkins, *J. Exp. Biol.* **202**, 1311 (1999).
11. B. A. Carlson, in *Communication in Fishes*, F. Ladich, S. P. Collin, P. Moller, B. G. Kapoor, Eds. (Science Publishers, Enfield, NH, 2006), vol. 2, pp. 805–848.
12. C. C. Bell, T. Szabo, in *Electroreception*, T. H. Bullock, W. Heiligenberg, Eds. (John Wiley & Sons, New York, 1986), pp. 375-421.
13. C. D. Hopkins, A. H. Bass, *Science* **212**, 85 (1981).
14. P. G. D. Feulner, M. Plath, J. Engelmann, F. Kirschbaum, R. Tiedemann, *Biol. Lett.* **5**, 225 (2009).
15. P. Machnik, B. Kramer, *J. Exp. Biol.* **211**, 1969 (2008).
16. M. E. Arnegard, B. S. Jackson, C. D. Hopkins, *J. Exp. Biol.* **209**, 2182 (2006).
17. A. H. Bass, in *Electroreception*, T. H. Bullock, W. Heiligenberg, Eds. (Wiley, New York, 1986), pp. 13–70.
18. H. H. Zakon, in *Electroreception*, T. H. Bullock, W. Heiligenberg, Eds. (Wiley, New York, 1986), pp. 103–156.
19. A. H. Bass, C. D. Hopkins, *J. Morphol.* **174**, 313 (1982).
20. W. Harder, *Z. Vgl. Physiol.* **59**, 272 (1968).
21. S. Lavoué, C. D. Hopkins, A. K. Toham, *Zoosystema* **26**, 511 (2004).
22. N. Post, G. von der Emde, *Physiol. Behav.* **68**, 115 (1999).
23. P. Moller, J. Serrier, D. Bowling, *Ethology* **82**, 177 (1989).
24. B. C. O'Meara, C. Ané, M. J. Sanderson, P. C. Wainwright, *Evolution* **60**, 922 (2006).
25. D. L. Rabosky, S. C. Donnellan, A. L. Talaba, I. J. Lovette, *Proc. Biol. Sci.* **274**, 2915 (2007).
26. M. J. Ryan, *Proc. Natl. Acad. Sci. U.S.A.* **83**, 1379 (1986).
27. O. Seehausen *et al.*, *Nature* **455**, 620 (2008).
28. Y. Terai *et al.*, *PLoS Biol.* **4**, e433 (2006).
29. J. B. Sylvester *et al.*, *Proc. Natl. Acad. Sci. U.S.A.* **107**, 9718 (2010).
30. C. A. Shumway, *Brain Behav. Evol.* **72**, 123 (2008).

Self-Organizing and Stochastic Behaviors During the Regeneration of Hair Stem Cells

Maksim V. Plikus,[1] Ruth E. Baker,[2] Chih-Chiang Chen,[1,3] Clyde Fare,[4] Damon de la Cruz,[1] Thomas Andl,[5] Philip K. Maini,[2,6] Sarah E. Millar,[7] Randall Widelitz,[1] Cheng-Ming Chuong[1,8]*

Stem cells cycle through active and quiescent states. Large populations of stem cells in an organ may cycle randomly or in a coordinated manner. Although stem cell cycling within single hair follicles has been studied, less is known about regenerative behavior in a hair follicle population. By combining predictive mathematical modeling with in vivo studies in mice and rabbits, we show that a follicle progresses through cycling stages by continuous integration of inputs from intrinsic follicular and extrinsic environmental signals based on universal patterning principles. Signaling from the WNT/bone morphogenetic protein activator/inhibitor pair is coopted to mediate interactions among follicles in the population. This regenerative strategy is robust and versatile because relative activator/inhibitor strengths can be modulated easily, adapting the organism to different physiological and evolutionary needs.

Continuous stem cell (SC) regeneration is essential for the maintenance of many adult organs, for example, in the bone marrow, skin, and gastrointestinal tract. Although regenerative behavior within a single SC cluster such as the hair bulge (*1*) or intestinal villi (*2*) has been studied, it is largely unknown how the regenerative behavior in populations of these SC clusters is coordinated. During development, thousands of cells can self-organize into anatomic structures and patterns by coordinating just a few morphogenetic signals (*3*), as seen in the periodic patterning of skin appendages (*4*, *5*). We hypothesize that the regenerative cycling of adult organ SCs can be similarly coordinated by diffusible signals and self-organize into spatiotemporal regenerative patterns.

Hair offers a suitable experimental model because hair follicles (HFs) cycle through phases of growth (anagen) and rest (telogen) (*6*). SCs are clustered in hair bulges, making them easier to study than SCs in other organs, where they are usually scattered randomly (*7*) (fig. S1A). Growing hairs produce pigmentation patterns that allow simultaneous monitoring of the regenerative behavior of thousands of SCs (Fig. 1A) (*8*, *9*). Additionally, the skin is flat, restricting interactions between HFs to two dimensions, further simplifying the analysis.

We developed a cellular automaton (CA) model consisting of a regular grid of automata, with one automaton representing one HF (fig. S1B) (*10*). The eight automata surrounding one automaton are defined as its neighbors. With time, the state of each automaton changes according to rules that take into account the state of neighboring automata. Automata in certain states can interact, generating complex, self-organizing patterns based on a simple set of rules. Such patterning behavior can be globally modulated by simple rule changes in local automaton-to-automaton interactions (*11*).

To form regenerative patterns, activating signals among SCs should be able to spread and stop. This is possible when SCs can differentially respond to the same signal at different times of their regenerative cycle. We previously identified four functional phases in the hair regenerative cycle: signal-propagating (P) and nonpropagating phases (A), and phases refractory (R) and competent (C) to such signals (*12*). Telogen HFs in R phase cannot enter anagen because bone morphogenetic proteins (BMPs) in the surrounding skin macroenvironment keep hair SCs quiescent (*12*). Telogen HFs in C phase are devoid of these inhibitors and can enter anagen as long as the sum of intrinsic and extrinsic activators is above the threshold. Intrinsic activators are produced as the result of hair SCs and dermal papilla interactions. Extrinsic activators come from neighboring P-phase anagen HFs and represent a form of collective positive feedback. Thus, HFs can enter anagen in two ways: autonomously, depending on the level of intrinsic activation, or nonautonomously, when activators are delivered by the surrounding macroenvironment. The probability of anagen entry is based on the sum of these fluctuating inputs.

We used mathematical simulations to test the sufficiency and robustness of this model. We show that the CA model encompassing P→A→R→C cycling can reproduce the full spectrum of hair regenerative patterns observed in mice: formation of initiation centers, wave spreading, maintenance of borders, and border instability (Fig. 1B, fig. S2, and table S1).

For a model to be robust and capture conserved patterning principles, it should be capable of explaining the diverse regenerative patterns seen in mutant mice and other animals. The duration of each phase of the regenerative cycle depends on the relative strengths of activators and inhibitors (Fig. 1A). We suggest that dif-

[1]Department of Pathology, University of Southern California (USC), Los Angeles, CA 90033, USA. [2]Centre for Mathematical Biology, Mathematical Institute, 24-29 St. Giles', Oxford OX1 3LB, UK. [3]Institute of Clinical Medicine and Department of Dermatology, National Yang-Ming University and Department of Dermatology, Taipei Veterans General Hospital, Taipei, Taiwan. [4]Life Sciences Interface Doctoral Training Centre, Wolfson Building, Parks Road, Oxford OX1 3QD, UK. [5]Vanderbilt University Medical Center, Nashville, TN 37232, USA. [6]Oxford Centre for Integrative Systems Biology, Department of Biochemistry, South Parks Road, Oxford OX1 3QU, UK. [7]Department of Dermatology, University of Pennsylvania, Philadelphia, PA 19104, USA. [8]Research Center for Developmental Biology and Regenerative Medicine, National Taiwan University, Taiwan.

*To whom correspondence should be addressed. E-mail: cmchuong@usc.edu